



Minerva Access is the Institutional Repository of The University of Melbourne

Author/s:

Wong, JWH;Plett, KL;Natera, SHA;Roessner, U;Anderson, IC;Plett, JM

Title:

Comparative metabolomics implicates threitol as a fungal signal supporting colonization of *Armillaria luteobubalina* on eucalypt roots

Date:

2020-02-01

Citation:

Wong, J. W. H., Plett, K. L., Natera, S. H. A., Roessner, U., Anderson, I. C. & Plett, J. M. (2020). Comparative metabolomics implicates threitol as a fungal signal supporting colonization of *Armillaria luteobubalina* on eucalypt roots. *Plant Cell and Environment*, 43 (2), pp.374-386. <https://doi.org/10.1111/pce.13672>.

Persistent Link:

<https://hdl.handle.net/11343/286709>

Comparative metabolomics implicates threitol as a fungal signal supporting colonization of *Armillaria luteobubalina* on eucalypt roots

Johanna W-H Wong¹, Krista L Plett¹, Siria H A Natera², Ute Roessner^{2,3}, Ian C Anderson¹, Jonathan M Plett^{1*}

¹Hawkesbury Institute for the Environment, Western Sydney University, Richmond NSW 2753, Australia

²Metabolomics Australia, The University of Melbourne, Parkville VIC 3010, Australia

³School of BioSciences, The University of Melbourne, Parkville VIC 3010, Australia

*** Correspondence:**

Jonathan M Plett

j.plett@westernsydney.edu.au

This is the author manuscript accepted for publication and has undergone full peer review but has not been through the copyediting, typesetting, pagination and proofreading process, which may lead to differences between this version and the [Version of Record](#). Please cite this article as doi: [10.1111/pce.13672](https://doi.org/10.1111/pce.13672)

1 **Abstract**

2 *Armillaria* root rot is a fungal disease that affects a wide range of trees and crops around the
3 world. Despite being a widespread disease, little is known about the plant molecular
4 responses towards the pathogenic fungi at the early phase of their interaction. With recent
5 research highlighting the vital roles of metabolites in plant root-microbe interactions, we
6 sought to explore the pre-symbiotic metabolite responses of *Eucalyptus grandis* seedlings
7 towards *Armillaria luteobuabulina*, a necrotrophic pathogen native to Australia. Using a
8 metabolite profiling approach, we have identified threitol as one of the key metabolite
9 responses in *E. grandis* root tips specific to *A. luteobubalina* that were not induced by three
10 other species of soil-borne microbes of different lifestyle strategies (a mutualist, a
11 commensalist, and a hemi-biotrophic pathogen). Using isotope labeling, threitol detected in
12 the *Armillaria*-treated root tips was found to be largely derived from the fungal pathogen.
13 Exogenous application of D-threitol promoted microbial colonization of *E. grandis* and
14 triggered hormonal responses in root cells. Together, our results support a role of threitol as
15 an important metabolite signal during eucalypt-*Armillaria* interaction prior to infection thus
16 advancing our mechanistic understanding on the earliest stage of *Armillaria* disease
17 development.

18
19 **Summary statement**

20 Comparative metabolomics of eucalypt roots interacting with a range of fungal lifestyles
21 identified threitol enrichment as a specific characteristic of *Armillaria* pathogenesis. Our
22 findings suggest that threitol acts as one of the earliest fungal signals promoting *Armillaria*
23 colonization of roots.

24
25 **Keywords:** plant-microbial interaction, rhizosphere, fungal tree pathogen, biomarkers,
26 metabolomics, GC-MS, disease detection, soil microbes
27

28 **Introduction**

29 *Armillaria* root disease is a ubiquitous root disease threatening numerous tree species in the
30 world including a wide range of eucalypt species. *Armillaria*-infected eucalypts usually show
31 symptoms such as white mycelical sheets under the bark, white rot of sapwood, black
32 rhizomorphs penetrating root surfaces and honey-coloured mushrooms clusters. Further
33 aboveground symptoms include reduced growth of the host, distress cone crop, and crown
34 thinning (Kile 2000). As *Armillaria* usually causes only a minor disturbance to native
35 eucalypts forests and plantations, these fungi are often considered as an unimportant,
36 indigenous soil-borne pathogen of eucalypts in Australia (Burgess & Wingfield 2004).
37 However, when trees are under stress due to drought or temperature extremes, they became
38 more prone to *Armillaria* disease (Sturrock *et al.* 2011). Therefore, in view of changing
39 global climatic conditions, root rot attributed to *Armillaria* infection could become more
40 prominent in the future.

41

42 Within the *Armillaria* genus, *Armillaria luteobubalina* is a particularly deadly species that
43 can cause root rot or even mortality among eucalypts in both native forests and plantations,
44 setting itself apart from other native *Armillaria* species in Australia (Kile 2000; Burgess &
45 Wingfield 2004). *A. luteobubalina* has been the major causal agent of dieback and decline of
46 eucalypts in central Victoria and south-western Australia in the last century (Kile 1981;
47 Robinson 2003). The current diagnostic strategy for *Armillaria* disease relies heavily on
48 visual inspection for the symptoms mentioned above, which are unfortunately similar to other
49 root diseases and usually only appear in the later stage of the disease, making *Armillaria*
50 disease difficult to detect (Kile 2000). Despite being a common tree disease, little is known
51 about the molecular pathways underlying the *Armillaria* disease development in eucalypts –
52 knowledge that could be critical to devising new methods for control of *Armillaria* root
53 infection. Transcriptomic analysis of *Armillaria* after colonization of grand fir (Ross-Davis *et al.*
54 *al.* 2013) and genomic and proteomic analysis of *A. mellea* (Collins *et al.* 2013) have
55 explored the contribution of digestive enzymes and effector proteins during degradation of
56 the plant tissues, yet the molecular mechanisms initiating the infection of *Armillaria* fungi on
57 tree roots are largely unknown. Better knowledge concerning the onset of *Armillaria*
58 infection in trees could aid more effective, proactive management of the disease.

59

60 Interactions between plants and soil microbes are often initiated by the exchange of
61 metabolite signals. While the majority of metabolites used as signals between organisms in
62 plant-microbe interactions are common to both mutualistic and pathogenic symbioses (Xu *et al.*
63 *et al.* 2015; Wong *et al.* 2019), there are also examples in the literature where either soil
64 microbes or their plant hosts release genus- or species-specific metabolites that facilitate their
65 interaction. For example, root exudate contents of tomato and tall fescue vary based on the
66 type of soil-microbes with which they were interacting (Kamilova, Kravchenko,
67 Shaposhnikov, Makarova & Lugtenberg 2006; Guo, McCulley & McNear 2015). Similarly,
68 soil-microbes can produce specific metabolites to facilitate root colonization on host plants;
69 the secretion of hypaphorine by the ectomycorrhizal fungus *Pisolithus tinctorius* is related to
70 colonization (Beguiristain & Lapeyrie 1997). These studies are, therefore, a proof of concept
71 demonstrating that a range of metabolites derived from either the plant or the interacting
72 microbe can be selectively present during plant-microbial interaction. Further, these studies
73 may indicate that the difference in plant metabolite responses towards different microbes
74 could be the key to determine the interaction outcome between the two organisms. Given
75 their key importance, these metabolite responses could also be used as ‘biomarkers’ to
76 indicate the health or disease status in plants and provide further insight into the
77 pathogenicity of the disease agent. Using gas chromatography-coupled mass spectrometry
78 (GC-MS), metabolite biomarkers have been identified for plant diseases such as *Tomato*
79 *yellow leaf curl virus* (Sade *et al.* 2014), *Ganoderma* disease in oil palm (Nusaibah, Siti Nor
80 Akmar, Idris, Sariah & Mohamad Pauzi 2016), and *Fusarium* infection in maize (Sherif *et al.*
81 2016). For *Armillaria* disease, pine seedlings infected with *A. ostoyae* exhibited distinct
82 levels of certain metabolites nine months post-inoculation despite there being no visible
83 symptoms (Isidorov, Lech, Żółciak, Rusak & Szczepaniak 2008). To further expand our
84 knowledge of the mechanisms regulating *Armillaria* pathogenicity, and to advance the
85 detection strategy of *Armillaria* root rot, we need to improve our understanding of the host
86 metabolite responses, and their underlying roles, during the early stages of the interaction.

87

88 In this study, we explore the metabolite response of *Eucalyptus grandis* roots towards *A.*
89 *luteobubalina* during the earliest phases of interaction (i.e. pre-symbiosis) in an effort to
90 advance our understanding of key metabolite signals underpinning the onset of *Armillaria*
91 disease in eucalypts. The root metabolite responses towards *A. luteobubalina* at 24 h pre-
92 symbiotic interaction (i.e. before the plants and fungi come into physical contact) were

93 profiled and compared to the metabolite profiles of eucalypt roots similarly exposed to three
94 other distinct groups of microbes— the mutualistic ectomycorrhizal fungus *Pisolithus*
95 *microcarpus*; the commensal fungus *Suillus granulatus* and the hemi-biotrophic oomycete
96 *Phytophthora cinnamomi*, in order to identify metabolite responses that are specific to the *E.*
97 *grandis*-*A. luteobubalina* interaction. We identify a number of metabolite responses specific
98 to the *Armillaria* interaction. We further characterize the role of one of these metabolites, D-
99 threitol, on *E. grandis* defence gene expression and on *Armillaria* infection efficiency.

100

101

102 **Materials and methods**

103 **Fungal culture condition**

104 A total of 10 different isolates of fungi corresponding to three fungal species representing
105 different lifestyles and one isolate of pathogenic oomycete *P. cinnamomi* were sampled from
106 several locations in New South Wales, Australia and used in this study (Table S1). Agar
107 plugs containing mycelium of each fungal isolates and oomycete isolate were grown on a
108 piece of permeable, sterile cellophane membrane (Kleerview Covers by Fowlers Vacola
109 Manufacturing Co Ltd.) in their preferred growth medium (Table S1). The fungal and
110 oomycete cultures were allowed to grow in a dark growth cabinet controlled at 25°C for 14 d
111 before the pre-symbiosis experiment with *E. grandis*.

113 **Plant growth condition**

114 To establish the experiment, *E. grandis* seeds (seedlot 20974) were obtained from the
115 Commonwealth Scientific and Industrial Research Organisation (CSIRO, Clayton, Victoria,
116 Australia) tree seed center. Seeds sterilization was performed by submerging the seeds in
117 30% (v/v) H₂O₂ for 10 min followed by washing in sterilized deionized water for 5 min five
118 times. After sterilization, seeds were germinated in 1% water agar for three weeks before
119 transferring into half-strength modified MMN media. The *E. grandis* seedlings were
120 cultivated in a controlled growth chamber (22-30°C; 16 h light cycle) for 1 month prior to the
121 pre-symbiotic interaction with microbes.

123 **Pre-symbiotic plant-microbial interaction set-up for untargeted metabolite profiling**

124 Both *E. grandis* seedlings, fungal cultures and oomycete cultures were allowed to acclimatize
125 to modified half-strength MMN media without glucose for 3 d before the set-up of the pre-
126 symbiotic interaction. At the beginning of the experiment, each cellophane membrane
127 containing the fungal/oomycete mycelia was placed on top of the root system of a *E. grandis*
128 seedling (2-month-old) whereby the cellophane membrane physically separated the
129 fungal/oomycete mycelia from the *E. grandis* root system but allowed diffusion of chemical
130 compounds between the microbe and the plant as per Wong et al. (2019). The 24 h pre-
131 symbiotic interaction was carried out in a controlled growth chamber (22-30°C; 16 h light
132 cycle) and root tips of *E. grandis* were sampled, subjected to snap-freezing with liquid N₂ and
133 stored in a -80°C freezer. An untreated seedling control was also set up (*E. grandis* seedlings

134 covered by sterile cellophane membrane). The frozen samples were sent to Metabolomics
135 Australia at the University of Melbourne for untargeted metabolite profiling using gas
136 chromatograph mass spectrometer (GC-MS) as described in Roessner *et al.* (2001). Details of
137 the sample preparation and analytical procedures are described in Supplementary Materials
138 and Methods. While GC-MS is not able to comprehensively profile the full suite of
139 metabolites within the root, it has the advantage of a high efficiency of peak separation and
140 reproducible retention times that enable it to be better compared to previously performed
141 research (Scalbert *et al.* 2009; Vinaixa *et al.* 2016). The ionization used in the method also
142 allows for standardized spectral fingerprints that increase the possibility of positive
143 identification against public databases. Conversely, the derivatization steps required for the
144 analysis mean that some compounds become too unstable and are therefore missed. Other
145 techniques could be used to generate a longer list of MFs, but as the aim of this paper was to
146 find a method that could be used comparably between laboratories and use as simple a
147 workflow as possible, thereby increasing the possible implementation as a potential screening
148 tool for disease in different settings, we chose to use the GC-MS platform.

149

150 **Soil-based *Armillaria*-treatment set up for untargeted metabolite profiling**

151 Two-month-old *E. grandis* seedlings growing on half-strength MMN media were transferred
152 individually into pots containing soil (Osmocote professional seed and cutting potting mix by
153 Evergreen Garden Care Australia Pty Ltd.) sterilized by autoclaving two times at 121°C for
154 three hours. The seedlings were then allowed to grow in soil for another month in a growth
155 chamber (22-30°C; 16 h light cycle). To allow soil-based interaction with *A. luteobubalina*,
156 the three-month-old *E. grandis* seedlings were transferred into a pot with 0.5 L of soil
157 inoculated with 25 mL of homogenized *A. luteobubalina* culture in PDA media. An
158 uninoculated control (0.5 L soil mixed with 25 mL of sterile PDA media) was also set up.
159 After 7 d of interaction in the abovementioned growth chamber, the soil was discarded from
160 the pot and the root tips of the *E. grandis* seedlings were harvested and immediately frozen in
161 liquid N₂. The frozen root tip samples were analyzed for metabolite profiles as above.

162

163 **Targeted D-threitol quantification throughout *A. luteobubalina* colonization of *E.*** 164 ***grandis* and under different nutrient regimes**

165 In order to understand the production of threitol throughout colonization, *E. grandis* and *A.*
166 *luteobubalina* were grown separately and pre-treated as above. Fungal cultures were then
167 placed into either indirect contact with *E. grandis* roots for 24hrs, as described above, or were
168 placed into direct physical contact. For the latter samples, at prescribed intervals (24hrs,
169 48hrs, 1 week, and 2 weeks) the roots and adherent fungi were separated and snap frozen in
170 liquid nitrogen and stored at -80°C until extraction and analysis. In order to understand if
171 nutrient levels in the growth medium may serve as a signal for threitol production, we grew *A.*
172 *luteobubalina* on a series of media with decreasing concentrations of potato dextrose (1x,
173 1/2x, 1/4x, and 1/10x) for 2 months after which fungal tissue samples were taken, snap frozen
174 and then analyzed for threitol concentration as below.

175
176 Because of different extraction efficiencies, we used two different methods to extract threitol
177 from roots and from fungi. For the roots, the fresh weight of the root tip samples were
178 recorded during harvest. Approximately 20-30mg of frozen root samples per biological
179 replicate were homogenized using a bead mill (FastPrep-24, MP Biomedicals, LLC) and then
180 incubated with 600µl of 60% (v/v) methanol (HPLC grade) in a thermomixer (Eppendorf) set
181 at 60°C with a mixing speed of 1,000 rpm for 30 min. The extracts were then centrifuged at
182 13,000 rpm for 5 min. Cleared supernatant samples were then collected and dried using a
183 vacuum concentrator (SpeedVac, Thermo Fisher Scientific) set at ambient temperature. The
184 dried extracts were re-suspended in 1/10 of the original volume of 60% (v/v) methanol and
185 stored at -20°C until analysis. For the fungal samples, the fresh weight of the fungal mycelia
186 samples were recorded during harvest. Frozen fungal samples were homogenized using a
187 bead mill (FastPrep-24, MP Biomedicals, LLC) and then incubated with 100µl per 10mg
188 fresh sample of pure methanol (HPLC grade) in a thermomixer (Eppendorf) set at 30°C with
189 a mixing speed of 1,000 rpm for 15 min. The methanol extracts were then centrifuged at
190 13,000 rpm for 5 min. Clarified supernatant samples were then collected and set aside in a
191 new microcentrifuge tube. 100µl per 10mg fresh samples of deionized water was added into
192 the sample pellet, vortexed for 10 sec and incubated at ambient temperature for 5 min. The
193 water extracts were then centrifuged at 13,000 rpm for 5 min. Clarified water extracts were
194 collected and mixed with the aforementioned methanol extracts, and dried using a vacuum
195 concentrator (SpeedVac, Thermo Fisher Scientific) set at ambient temperature. The dried
196 extracts were re-suspended in 1/5 of the original volume of 50% (v/v) methanol and stored at
197 -20°C until analysis.

198

199 Of each sample, 2µl was injected into the Agilent 1260 Infinity HPLC-system equipped with
200 a Shodex Asahipak NH2P-50 4E column (4.6 x 250 mm, 5µm) warmed at 55°C, and a
201 Dionex Corona charged aerosol detector (CAD). The mobile phase was optimized based on
202 the sample types. Elution was done isocratically with 1:1 (v/v) deionized water: acetonitrile
203 (HPLC grade) for root samples, whereas 1:4 (v/v) deionized water: acetonitrile (HPLC grade)
204 was used for fungal samples. In both cases, the elution was done at the rate of 1.2mL/min for
205 10min. A set of seven D-threitol standards at concentrations ranging from 250ppm to
206 4,000ppm were used to identify and quantify the concentration of threitol in each sample. The
207 resulting quantitation was normalized based on the fresh weight of each sample.

208

209 **Statistical analysis of metabolite profiling data**

210 The metabolite profiling data matrix, containing the relative response ratios of each
211 metabolite (including both identified and unknown metabolites) in each condition, was
212 loaded on the R platform (version 3.5.1). Data transformation (log-transformation and auto-
213 scaling), univariate analysis and principle component analysis (PCA) were performed with
214 MetaboAnalystR (version 1.0.1) with the metabolite profiling data matrix. Recursive
215 partitioning and regression tree (rpart) and parallel random forest (parRF) were performed
216 using the caret package (version 6.0-81) while sparse partial least square-discriminative
217 analysis (sPLS-DA) was carried out with mixOmics (version 6.6.0) package on R. The
218 workflow of this analysis can be found in Figure S1.

219

220 **Threitol quantitation, ¹³C-isotopic labelling and tracing**

221 Prior to pre-symbiotic interaction with *E. grandis*, *A. luteobubalina* and *P. microcarpus* were
222 labelled with ¹³C by growing the fungi on modified half-strength MMN agar media with 1
223 g/L of 99% ¹³C₆-glucose (Cambridge Isotope Laboratories, Inc.) for one month. An
224 unlabelled control was also prepared. The fungal cultures were then transferred to half-
225 strength MMN media (without glucose) for 3 d, followed by pre-symbiotic interaction with *E.*
226 *grandis* seedlings for 24 h as described above. Root tip samples and fungal mycelia were
227 collected and snap-frozen in liquid N₂, and subsequently stored in -80 °C freezer until
228 extraction and metabolite analysis by Metabolomics Australia at the University of Melbourne.
229 Untargeted metabolite profiling, threitol ¹³C isotope enrichment analysis, as well as targeted
230 quantitation of threitol were performed as described in Roessner *et al.* (2001), Nanchen,

231 Fuhrer & Sauer (2007) and Dias *et al.* (2015) respectively. Detailed procedures can be found
232 in Supplementary Materials and Methods.

233

234 **Threitol treatment and microbial infection assay**

235 To identify the impact of D-threitol on the rate of microbial infection, one-month-old mycelia
236 of *A. luteobubalina*, one-week-old hyphae of *Ph. cinnamomi*, or two-week-old mycelia of *P.*
237 *microcarpus* isolate SI-14 were placed directly onto *E. grandis* roots on three types of half-
238 strength MMN agar media with different D-threitol concentrations – 0 ppm, 0.3 ppm and 12
239 ppm, and co-cultured for 14 d in a growth chamber set at the growth conditions described
240 above. These D-threitol concentrations were chosen based the quantified ranges of the
241 metabolite in the roots of *E. grandis* across all of our experiments. Sterile *E. grandis*
242 seedlings monoculture growing on media of the same threitol concentration was set up
243 alongside as a negative control. After 14 d, the lateral roots were observed under a
244 stereoscope and degree of infection/colonization were counted manually for *E. grandis*
245 seedlings. Infection for the two pathogens was classified as the percentage of root lesions
246 caused by either *A. luteobubalina* or *Ph. cinnamomi* divided by the total number of lateral
247 roots in contact with fungal mycelium. For the mutualistic fungus *P. microcarpus* isolate SI-
248 14, the percentage of colonized root tips was compared between each treatment.

249

250 **Electrolyte Leakage**

251 As a secondary means to quantify damage to the roots caused by *A. luteobubalina* over time,
252 we measured electrolyte leakage of infected roots across the timecourse of colonization (i.e.
253 from pre-contact through 2 weeks post-contact). For these assays, 2-4 lateral roots in contact
254 with *A. luteobubalina* were excised and placed in 3 mL of Milli-Q water and left to incubate
255 at 25°C for 1 hour. After this incubation, the conductivity of the water was measured using a
256 conductivity meter. The samples were then boiled at 95°C for one hour followed by cooling
257 of the sample back to 25°C. Following temperature equilibration, conductivity was again
258 measured and the percentage of the first reading versus the second reading was recorded. An
259 average of four biological replicates were performed per data point.

260

261 **RNA extraction and real-time quantitative PCR (RT-qPCR) assay**

262 *E. grandis* seedlings were transferred onto half-strength MMN agar media supplemented with
263 0 ppm or 12 ppm D-threitol. After 24 hours, the plant roots were harvested and three
264 biological replicates from each condition were immediately frozen in liquid nitrogen. RNA
265 was extracted from the roots with the Bioline Isolate II miRNA extraction kit. Extracted
266 RNA was used as a template for cDNA synthesis using the Bioline SensiFAST cDNA
267 synthesis kit. RT-qPCR analysis was conducted on a BioRad CFX96 Touch RT-PCR cyclor
268 using the Bioline SensiFAST SYBR No-ROX kit. Log₂ fold change of gene expression of 12
269 ppm D-threitol treated roots as compared to control roots (0 ppm D-threitol) was calculated
270 for the closest *E. grandis* homologues to known Arabidopsis hormone responsive genes:
271 ABI3 (*Eucgr.H00815*), PIN1 (*Eucgr.K02271*), PIN2 (*Eucgr.C00078*), PIN3 (*Eucgr.B02902*),
272 ARR16 (*Eucgr.G03141*), ARR6 (*Eucgr.B02571*), GA3ox1 (*Eucgr.F02568*), Myc2
273 (*Eucgr.E00277*) and VSP2 (*Eucgr.J02927*). RT-qPCR gene expression results were
274 normalized using *Eucgr.C00350* and *Eucgr.B03031* as control genes. Primers used in the RT-
275 qPCR assays are listed in the Table S2. To understand if the impact of D-threitol on the
276 transcriptomic expression of these hormone-responsive genes was specific to this compound
277 or if it was a general response to different sugar compounds, we also exposed a second set of
278 *E. grandis* seedlings to the sugar myo-inositol at either 0 or 25 ppm for 24 hr. RNA was then
279 extracted from these root systems, followed by cDNA synthesis and RT-qPCR performed on
280 the same genes as above.

281

282 **Results**

283 **Metabolite responses of *E. grandis* root tips during pre-symbiosis with *A. luteobubalina***

284 With GC-MS based untargeted metabolite profiling, a total of 117 metabolites were detected
285 in *E. grandis* root tips when grown axenically, including 67 identifiable metabolites and 50
286 unknown metabolites (Table S3). After 24 h of pre-symbiotic ‘indirect’ contact with *A.*
287 *luteobubalina* (i.e. plant and fungus were allowed to exchange diffusible signals but were
288 physically separated by a membrane), 13 metabolites in *E. grandis* root tips were increased in
289 abundance by more than two-fold. Apart from the unknown metabolites, the highly repressed
290 root metabolite responses (fold change < 0.5) mostly belong to organic acids while the
291 majority of highly enriched metabolites (fold change >2) are either sugars, sugar alcohols,
292 amines or amino acids (Table 1; Full list of root metabolite responses towards *A.*
293 *luteobubalina* are listed in Table S4). Mannitol, trehalose and threitol exhibited the most
294 significant enrichment in *E. grandis* roots upon interaction with *A. luteobubalina* (Figure 1).

295

296 In order to understand which of the metabolite responses by *E. grandis* might be specific to
297 contact with *A. luteobubalina*, we compared the *E. grandis* root metabolite responses
298 described above with root metabolite responses to three other species of soil microbes
299 commonly found in eucalypt forests in Australia, including the pathogenic oomycete
300 *Phytophthora cinnamomi*, the commensal fungus *Suillus granulatus*; and the mutualistic
301 ectomycorrhizal fungus, *Pisolithus microcarpus*. Principle component analysis (PCA) could
302 not clearly separate the metabolite profiles of *E. grandis* root tips based on the microbial
303 treatment (Figure 2), although permutational multivariate analysis of variance
304 (PERMANOVA) indicated that the microbial treatments have significant effect on *E. grandis*
305 root metabolite profiles ($p < 0.001$) whereby 20.58% of the variance in the metabolite
306 responses can be explained by the different species of interacting microbes. Our results
307 suggest that the overall metabolite responses of *E. grandis* roots are non-random and that
308 certain root metabolites respond selectively towards different species of microbes.

309

310 **Identification of *Armillaria*-specific metabolite responses in *E. grandis* root tips**

311 To identify potential metabolites in *E. grandis* root tips that are specific to the interaction
312 with *A. luteobubalina*, we made use of supervised machine learning (ML) models. Three ML

313 models – parallel random forest (parRF), sparse partial least square discriminative analysis
314 (sPLSDA) and recursive partitioning and regression tree (rpart) – were trained with a subset
315 of our metabolomics datasets (n = 36) to select important metabolite responses with high
316 discriminative power that effectively split the root metabolite profiles into three groups: *A.*
317 *luteobubalina*-treated group (*Armillaria*), untreated control group (Control) or other
318 microbial treatments (Other). The accuracy of each of the three ML models were evaluated
319 by cross-validation and fine-tuning of parameters to optimize their performance (Table 2).
320 Prediction performance of each model was validated externally with a subset of the data (n =
321 12) that was previously omitted for testing purposes (Table 2). With the AUROC index
322 approaching 1, the performance testing result ensured a high confidence was accrued by our
323 ML models.

324
325 The top ten important metabolite responses with the highest discriminative capacities were
326 selected by each of the ML models (Figure 3a). Threonic acid, shikimic acid, threitol, lactic
327 acid and inositol were commonly selected by the three MS models as the most important
328 features for classification between *Armillaria*, Control and Other (Figure 3b). These three
329 classification groupings could also be effectively separated when the responses of these
330 important metabolites (threonic acid, shikimic acid, threitol, lactic acid and inositol) were
331 considered together (Figure 3c). Threitol was the only discriminatory metabolite induced in
332 the *Armillaria* group but not the other groups, while the other four aforementioned metabolite
333 responses were repressed in *Armillaria* and Other in comparison to Control (Figure 3b). In a
334 separate, targeted threitol quantitation analysis, we found that the quantity of D-threitol in
335 root tips treated with *A. luteobubalina* was > 20 times higher than in root tips treated with *P.*
336 *microcarpus* (Table 3). Given the strong explanatory value of threitol from these results, we
337 wished to see if it was also present in *E. grandis* root tips when they were exposed to
338 *Armillaria* in a system that more closely resembled a natural system (i.e. a soil-based system).
339 We found that the enrichment of threitol was also observed in *E. grandis* root tips in this soil-
340 based setup, but only when *Armillaria* was present (Figure 4).

341

342 **Threitol detected in *E. grandis* root tips is largely of fungal origin**

343 As we identified threitol to be significantly enriched on root tips when *E. grandis* interacts
344 with *A. luteobubalina*, we sought to ascertain the origin of the threitol—whether it was a

345 fungal-derived metabolite that diffused to *E. grandis* roots, or a plant-synthesized metabolite.
346 Therefore, we used an isotope labelling experimental setup to separate fungal-derived
347 metabolites from plant-derived metabolites. By culturing *A. luteobubalina* on $^{13}\text{C}_6$ -glucose
348 spiked media for a month, we successfully enriched the proportion of ^{13}C -labelled threitol
349 amongst all detectable isotopomers in the fungal mycelium, especially the $^{13}\text{C}_3$ -threitol
350 (derivative $m/z = 220$) and $^{13}\text{C}_4$ -threitol (derivative $m/z = 221$) isotopomers (Figure 5). In
351 these samples, ^{13}C -labelled isotopomers made up >55% of the total threitol abundance. In
352 comparison, threitol detected when *A. luteobubalina* was grown on a substrate without ^{13}C
353 enrichment, had a significantly lower percentage of ^{13}C -labelled isotopomers. When *E.*
354 *grandis* root tips were placed into pre-symbiotic interaction with the ^{13}C -labelled *A.*
355 *luteobubalina* mycelium, >40% of the total threitol recovered in the root tips was labelled
356 with ^{13}C . These results demonstrate that *A. luteobubalina* is able to synthesize its own threitol
357 and suggests that the majority of threitol detected *E. grandis* root tips during pre-symbiosis
358 originated from *A. luteobubalina*.

359

360 **Threitol production occurs prior to cell damage and under nutrient limited conditions**

361 To gain insight into the production of D-threitol in *A. luteobubalina* during colonization of *E.*
362 *grandis*, and to understand the uptake of this compound in plant tissues in relation to disease
363 progression, we quantified D-threitol in both the fungal tissues and the plant root across
364 colonization. As shown in Figure 6a, D-threitol was found in *A. luteobubalina* tissues at very
365 high concentrations prior to contact when grown on glucose-free medium (i.e. timepoint '0')
366 and for the first 24hrs of interaction between the two organisms be that pre-symbiotic
367 interaction or direct plant-fungal contact. After 24hrs, fungal production of D-threitol began
368 to significantly decrease until it reached its lowest detected concentration at 2 weeks post-
369 contact with the host roots. In *E. grandis*, D-threitol root concentrations prior to the
370 interaction with *A. luteobubalina* was near the detection limit of the machine (Figure 6a).
371 These concentrations rose steadily through 24hrs of direct physical contact between the two
372 organisms after which root-associated D-threitol decreased slightly, but maintained a higher
373 than control level across fungal colonization of root tissues. It was interesting to note, based
374 on the measurement of ion leakage as a proxy for cell damage, that while D-threitol
375 accumulation in the fungus was at its highest, plant cell damage was at its lowest (Figure 6b).

376 It was not until the 1 week timepoint and beyond that we observed significant increases in
377 cell damage.

378

379 As D-threitol concentrations in fungal tissues was highest prior to extensive root damage, and
380 because D-threitol concentration tailed off while root damage increased, this led us to
381 question whether D-threitol production may be controlled by fungal nutrition. To test this,
382 we grew *A. luteobubalina* on different concentrations of PDA. We found that D-threitol was
383 accumulated at high levels in fungal hyphae when grown on medium with lower levels of
384 nutrition than the fungus grown on 1x PDA (Figure 6c). Therefore the nutritional status of
385 the fungal colony impacts the synthesis of D-threitol.

386

387 **External treatment with threitol enhances microbial infection of *E. grandis* root tips**

388 Given the fact that *Armillaria* produces threitol during the early stages of colonization, which
389 coincides with the establishment phase of the fungus within the root system rather than the
390 root damage phase (Figure 6A,B), we evaluated the effect of increased threitol levels upon
391 the colonization ability of *A. luteobubalina* when in contact with *E. grandis* roots. Exogenous
392 application of even very low levels of threitol enhanced root lesions caused by *A.*

393 *luteobubalina*; a significant increase of ~10% and 25% by threitol treatment of 0.3 ppm and
394 12 ppm, respectively, was observed (Figure 7a). To understand if this phenomenon was
395 specific to *A. luteobubalina* colonization, or if the impact were more general, we also tested
396 the impact of exogenous D-threitol application on the colonization by either *Ph. cinnamomi*
397 or of *P. microcarpus*. We found that lesion development of roots colonized by *Ph.*
398 *cinnamomi* was increased significantly when low amounts of D-threitol were supplied, but
399 that this effect was reduced at higher levels of D-threitol (Figure 7b). Colonization of roots
400 by the mutualistic fungus *P. microcarpus* was significantly enhanced at both levels of D-
401 threitol tested (Figure 7c). Therefore, this metabolite signal can improve general microbial
402 colonization of root tissues, although not as strongly as the impact on *A. luteobubalina*
403 disease expression.

404

405 **External treatment with threitol alters transcription of hormone-responsive genes**

406 As plant hormones are closely tied to colonization success of fungi (Chanclud & Morel 2016),
407 we sought to examine the transcriptional changes of a selection of hormone-responsive
408 marker genes in *E. grandis* by quantitative real-time PCR (qRT-PCR; Sarnowska *et al.* 2016).
409 As shown in Figure 8a, threitol treatment significantly induced expression of all tested
410 marker genes responsive to phytohormones including gibberellins (GA), jasmonic acid (JA),
411 cytokinin (CK), auxin and abscisic acid (ABA). This was a surprising result given the fact
412 that some of these pathways act in an antagonistic manner to each other. We, therefore,
413 tested another one of the discriminatory metabolites from our profiling described above,
414 myo-inositol, to determine if this response was just a stress response. We exposed the *E.*
415 *grandis* root system to myo-inositol as we did for D-threitol and analysed expression of these
416 same hormone responsive genes. In general, myo-inositol did not have any effect on the
417 expression level of these genes with the exception of PIN2 (Figure 8b). Therefore, other
418 metabolites found to be altered during the pre-symbiotic stage of *A. luteobubalina* disease
419 progression have different impacts on plant signalling pathways.

420

421

422 Discussion

423 The metabolic regulation during plant-microbe interactions could be crucial in determining
424 the outcome of the interaction ((Buee, Rossignol, Jauneau, Ranjeva & Bécard 2000; Akiyama,
425 Matsuzaki & Hayashi 2005; Steinkellner *et al.* 2007; Stuttmann *et al.* 2011; Lahrmann *et al.*
426 2013; Tschaplinski *et al.* 2014). *Armillaria* root rot is not only a widespread eucalypt tree
427 disease endemic to Australia, but also a promiscuous root disease infecting numerous species
428 of forest trees and crops worldwide (Baumgartner, Coetzee & Hoffmeister 2011). The
429 *Armillaria* enzymatic activities contributing to its pathogenicity, as well as the plant
430 metabolite responses towards *Armillaria* post-infection have previously been reported
431 (Isidorov *et al.* 2008; Ross-Davis *et al.* 2013). However, our understanding on the *in plantae*
432 molecular pathways initiating the *Armillaria*-plant interaction is still being developed and
433 knowledge of specific metabolite profiles characteristic of *A. luteobubalina* pathogenicity are
434 needed. In this study, we have demonstrated metabolite responses in eucalypt root tips as
435 early as 24 h after pre-symbiotic interaction with *A. luteobubalina*. Mannitol, threitol, and
436 trehalose appear to be among the most significantly enriched metabolites in *A. luteobubalina*-
437 treated roots. While the role of threitol in plant-fungal interaction has not yet been reported,
438 both mannitol and trehalose synthesis are known biotic stress responses of plants towards
439 fungal attack (Fernandez, Béthencourt, Quero, Sangwan & Clément 2010; Patel &
440 Williamson 2016). Our findings suggest that these previously described metabolite responses
441 of a plant host in response to fungal pathogens may be detectable after even very short
442 periods of interaction with the pathogen, and that such regulation could be triggered solely by
443 the exchange of metabolite signals without the need of physical contact.

444

445 Beyond their role in pathogenicity, metabolites have emerged as effective measures of plant
446 performance and as biomarkers of disease during plant-microbe interactions (Sankaran,
447 Mishra, Ehsani & Davis 2010; Fernandez *et al.* 2016). A good biomarker should achieve both
448 high sensitivity and specificity for robust indication of the plant disease (Nagana Gowda &
449 Raftery 2013). Studying the specificity of plant metabolite responses could thus benefit both
450 our basic knowledge of *Armillaria* disease and also the development of biomarkers for its
451 early detection. In this study, not only have we identified the early metabolite responses of *E.*
452 *grandis* towards *A. luteobubalina* prior to infection, but these metabolite profiles were also
453 compared with roots exposed to representatives of fungi from other lifestyles—mutualist (*P.*

454 *microcarpus*), ‘commensalist’ (*S. granulatus*) and hemi-biotrophic pathogen (*Ph. cinnamomi*)
455 under the exact same conditions. Our results showed that the overall metabolite profiles of
456 eucalypt roots after different microbial pre-symbiotic treatment was highly-overlapping,
457 suggesting that there are common innate metabolite responses common to this very early
458 stage of interaction regardless of the microbial species present. This observation is aligned
459 with a study by Müller *et al.* (2013), which showed a large number of common volatile
460 organic compounds emitted by both ectomycorrhizal fungi, pathogenic fungi and saprophytic
461 fungi. To separate metabolite responses specific towards *A. luteobubalina* from common
462 responses towards other microbial species, we employed an emerging tool for selection of
463 important features in metabolomic studies –machine learning models (Poezevara *et al.* 2017;
464 Shiokawa, Date & Kikuchi 2018). The three ML models used in this study were able to
465 identify a panel of important features that differentiate root metabolite responses of the
466 *Armillaria* interaction from other microbial interactions or the axenically grown control plant.
467 We have selected threitol among the important features for further characterization as it is
468 strongly induced in the *Armillaria* interaction. It is possible that additional untargeted
469 metabolomic methods (e.g. LC-MS/MS) would identify further life-style or fungal-specific
470 metabolite signals, but our work stands as a proof of concept that we can use even the
471 simplified approach of standard GC-MS analysis for identifying specific metabolites that are
472 linked to root colonization by a specific pathogen. Given that our comparative approach has
473 taken the interaction of a host with microbial species of other lifestyles into consideration,
474 these current results indicate that threitol is a promising biomarker specific for *Armillaria*
475 infection of *E. grandis* roots.

476

477 Threitol, a four-carbon sugar alcohol, has been detected in plant species such as *Nicotiana*
478 *tabacum* and *Coffea arabica*, as well as in mycelia of *Armillaria* fungal species (Birkinshaw,
479 Stickings & Tessier 1948; Martins, Araújo, Tohge, Fernie & DaMatta 2014; Hacham,
480 Matityahu & Amir 2017). Hence, it was unclear whether the threitol detected in the *E.*
481 *grandis* roots with the current study was derived from the fungal pathogen or the *E. grandis*
482 itself. By determining the isotopic composition of threitol in *E. grandis* root tissue after
483 interaction with ¹³C-labelled *A. luteobubalina*, we identified that threitol detected in root
484 tissues were ¹³C-enriched—meaning that it is chiefly secreted by *A. luteobubalina* and
485 translocated to *E. grandis* root tissues. This conclusion was further reinforced when
486 comparing the relative concentration differences of D-threitol in between *A. luteobubalina*

487 and *E. grandis* across all of the colonization timecourse (Figure 6). Specifically, D-threitol
488 levels in the roots followed fungal production levels, albeit at a lower concentration than in
489 fungal tissues. It is also interesting to note that fungal production of D-threitol may be
490 nutritionally regulated. In both culturing conditions, and during the stage when *A.*
491 *luteobubalina* would be recovering nutrients from its host (i.e. >48hrs when ion leakage
492 increases) we observe that D-threitol production decreases. Therefore, this is not only a
493 signal produced by *A. luteobubalina*, but it is perhaps also related to enhancing nutrient
494 acquisition by the fungus.

495

496 The function and metabolic pathway of threitol in either plants or fungi remain obscure
497 despite being a natural product of both. Therefore, it is currently impossible to follow the
498 transcriptomic expression patterns of threitol-related biosynthetic genes nor to make fungal
499 mutants that produce less threitol. Threitol was found to be a derivative of sorbose in plants
500 (McComb & Rendig 1963), a stereoisomer of erythritol in *Armillaria mellea* (Birkinshaw *et*
501 *al.* 1948), and a precursor of erythrulose and erythrose in bacteria *Mycobacterium smegmatis*
502 (Huang *et al.* 2015). The effect of fungal-derived threitol on plant roots has hitherto been
503 undescribed. We have tested the effect of threitol on hormonal responses and microbial
504 colonization in *E. grandis*. Our findings indicate induced expression of hormone-responsive
505 genes in roots towards gibberellins, jasmonic acid, cytokinin, auxin and abscisic acid upon
506 threitol treatment, an effect that was not observed when myo-inositol, one of the other
507 *Armillaria*-specific metabolites was also exposed to *E. grandis* roots. In spite of its large
508 impact of a wide range of hormonal pathways in the plant, colonization of *A. luteobubalina*
509 appears to be favored by exogenous threitol treatment. This colonization promotion was also
510 observed to a lesser extent when *E. grandis* was placed into contact with either *Ph.*
511 *cinnamomi* or *P. microcarpus*. These results suggest that while threitol may be produced by
512 *A. luteobubalina* to foster colonization, this metabolite may alter plant immunity in general
513 way that can benefit more than just *Armillaria* colonization. More research on the specific
514 mechanism of threitol's action during plant-microbe interactions will be necessary in future.

515

516 Our study has advanced our understanding of the pre-symbiotic metabolite regulation in *E.*
517 *grandis* prior to infection by *A. luteobubalina*. We identified threitol enrichment as an
518 important early stage metabolite in the *Armillaria*-induced response and highlighted the

519 potential of threitol as a biomarker for *Armillaria* disease detection. In addition, our study
520 provides insight into the promotional effect of threitol on root colonization by varying
521 microbes in *E. grandis*. Given that *Armillaria* species are found in major forest ecosystems
522 globally, further investigation should follow to better our understanding of the role of their
523 metabolites in pathogenicity and soil ecology.

524

525 **Acknowledgements**

526 JW would like to acknowledge the Western Sydney University for a PhD research
527 scholarship and the North Shore District Group of the Australian Plants Society for the
528 Valette Williams Scholarship in Botany to support this research project. JP would like to
529 acknowledge the Australian Research Council for research funding (DE150100408). We
530 would also thank J. Rigg, E. Liew, and M. Laurence of the Botanic Gardens & Centennial
531 Parklands for providing isolates of *A.luteobubalina* and *Phytophthora cinnamomi* and S.
532 Hortal for providing isolates of *A. luteobubalina* and *S. granulatus*. The metabolite analyses
533 were conducted at Metabolomics Australia (School of BioSciences, The University of
534 Melbourne, Australia), a National Collaborative Research Infrastructure Strategy initiative
535 under Bioplatforms Australia Pty Ltd. We would like to acknowledge V. Liu, K. Kwan, H.
536 Mendis and N. Jayasinghe from the Metabolomics Australia for their contribution on the
537 metabolite analyses involved in this study.

538

539 **Conflict of interest**

540 The authors declare that they have no conflict of interest.

541

542 **References:**

- 543 Baumgartner K., Coetzee M.P.A. & Hoffmeister D. (2011) Secrets of the subterranean
544 pathosystem of *Armillaria*. *Molecular Plant Pathology* **12**, 515–534.
- 545 Beguiristain T. & Lapeyrie F. (1997) Host plant stimulates hypaphorine accumulation in
546 *Pisolithus tinctorius* hyphae during ectomycorrhizal infection while excreted fungal
547 hypaphorine controls root hair development. *New Phytologist* **136**, 525–532.
- 548 Birkinshaw J.H., Stickings C.E. & Tessier P. (1948) Biochemistry of the wood-rotting fungi:
549 5. The production of d-threitol (l-erythritol) by *Armillaria mellea* (Vahl) Quélet.
550 *Biochemical Journal* **42**, 329.
- 551 Burgess T. & Wingfield M.J. (2004) Impact of fungal pathogens in natural forest ecosystems:
552 a focus on eucalypts. in *Microorganisms in Plant Conservation and Biodiversity*. (eds
553 K. Sivasithamparama, K.W. Dixon & R.L. Barrett), pp. 285–306. Kluwer Academic
554 Publishers, Dordrecht.
- 555 Chanclud E. & Morel J.-B. (2016) Plant hormones: a fungal point of view. *Molecular Plant
556 Pathology* **17**, 1289–1297.
- 557 Collins C., Keane T.T.M., Turner D.J., O’Keeffe G., Fitzpatrick D. a & Doyle S. (2013)
558 Genomic and proteomic dissection of the ubiquitous plant pathogen, *Armillaria
559 mellea*: toward a new infection model system. *Journal of Proteome Research* **12**,
560 2552–70.
- 561 Dias D.A., Hill C.B., Jayasinghe N.S., Atieno J., Sutton T. & Roessner U. (2015)
562 Quantitative profiling of polar primary metabolites of two chickpea cultivars with
563 contrasting responses to salinity. *Journal of Chromatography B* **1000**, 1–13.
- 564 Fernandez O., Béthencourt L., Quero A., Sangwan R.S. & Clément C. (2010) Trehalose and
565 plant stress responses: friend or foe? *Trends in Plant Science* **15**, 409–417.
- 566 Fernandez O., Urrutia M., Bernillon S., Giauffret C., Tardieu F., Le Gouis J., ... Gibon Y.
567 (2016) Fortune telling: metabolic markers of plant performance. *Metabolomics* **12**.
- 568 Guo J., McCulley R.L. & McNear D.H.J. (2015) Tall fescue cultivar and fungal endophyte
569 combinations influence plant growth and root exudate composition. *Frontiers in Plant
570 Science* **6**.
- 571 Hacham Y., Matityahu I. & Amir R. (2017) Transgenic tobacco plants having a higher level
572 of methionine are more sensitive to oxidative stress. *Physiologia Plantarum* **160**,
573 242–252.
- 574 Huang H., Carter M.S., Vetting M.W., Al-Obaidi N., Patskovsky Y., Almo S.C. & Gerlt J.A.
575 (2015) A general strategy for the discovery of metabolic pathways: d-Threitol, l-
576 Threitol, and Erythritol utilization in *Mycobacterium smegmatis*. *Journal of the
577 American Chemical Society* **137**, 14570–14573.
- 578 Isidorov V.A., Lech P., Żółciak A., Rusak M. & Szczepaniak L. (2008) Gas
579 chromatographic–mass spectrometric investigation of metabolites from the needles
580 and roots of pine seedlings at early stages of pathogenic fungi *Armillaria ostoyae*
581 attack. *Trees* **22**, 531.
- 582 Kamilova F., Kravchenko L.V., Shaposhnikov A.I., Makarova N. & Lugtenberg B. (2006)
583 Effects of the tomato pathogen *Fusarium oxysporum* f. sp. radialis-lycopersici and of
584 the biocontrol bacterium *Pseudomonas fluorescens* WCS365 on the composition of
585 organic acids and sugars in tomato root exudate. *Molecular Plant-Microbe
586 Interactions* **19**, 1121–1126.
- 587 Kile G.A. (1981) *Armillaria luteobubalina* a primary cause of decline and death of trees in
588 mixed species eucalypt forests in central Victoria. *Australian Forest Research* **11**, 63–
589 77.

- 590 Kile G.A. (2000) Woody root rots of eucalypts. *Diseases and pathogens of eucalypts* (Eds. PJ
591 Kean, GA Kile, FD Podger and BN Brown), pp. 293–306. CSIRO publishing,
592 Australia
- 593 Lahrman U., Ding Y., Banhara A., Rath M., Hajirezaei M.R., Döhlemann S., ... Zuccaro A.
594 (2013) Host-related metabolic cues affect colonization strategies of a root endophyte.
595 *Proceedings of the National Academy of Sciences* **110**, 13965–13970.
- 596 Martins S.C.V., Araújo W.L., Tohge T., Fernie A.R. & DaMatta F.M. (2014) In high-light-
597 acclimated coffee plants the metabolic machinery is adjusted to avoid oxidative stress
598 rather than to benefit from extra light enhancement in photosynthetic yield. *PLOS*
599 *ONE* **9**, e94862.
- 600 McComb E.A. & Rendig V.V. (1963) Isolation and identification of L-threitol from plants
601 fed L-sorbose. *Archives of Biochemistry and Biophysics* **103**, 84–86.
- 602 Müller A., Faubert P., Hagen M., zu Castell W., Polle A., Schnitzler J.-P. & Rosenkranz M.
603 (2013) Volatile profiles of fungi – Chemotyping of species and ecological functions.
604 *Fungal Genetics and Biology* **54**, 25–33.
- 605 Nagana Gowda G.A. & Raftery D. (2013) Biomarker discovery and translation in
606 metabolomics. *Current Metabolomics* **1**, 227–240.
- 607 Nanchen A., Fuhrer T. & Sauer U. (2007) Determination of metabolic flux ratios from ¹³C-
608 experiments and gas chromatography-mass spectrometry data: protocol and principles.
609 *Methods in Molecular Biology (Clifton, N.J.)* **358**, 177–197.
- 610 Nusaibah S.A., Siti Nor Akmar A., Idris A.S., Sariah M. & Mohamad Pauzi Z. (2016)
611 Involvement of metabolites in early defense mechanism of oil palm (*Elaeis guineensis*
612 Jacq.) against Ganoderma disease. *Plant Physiology and Biochemistry* **109**, 156–165.
- 613 Patel T.K. & Williamson J.D. (2016) Mannitol in plants, fungi, and plant–fungal interactions.
614 *Trends in Plant Science* **21**, 486–497.
- 615 Poezevara G., Lozano S., Cuissart B., Bureau R., Bureau P., Croixmarie V., ... Lepailleur A.
616 (2017) A computational selection of metabolite biomarkers using emerging pattern
617 mining: a case study in human hepatocellular carcinoma. *Journal of Proteome*
618 *Research* **16**, 2240–2249.
- 619 Robinson R.M. (2003) Short-term impact of thinning and fertilizer application on *Armillaria*
620 root disease in regrowth karri (*Eucalyptus diversicolor* F. Muell.) in Western
621 Australia. *Forest Ecology and Management* **176**, 417–426.
- 622 Roessner U., Luedemann A., Brust D., Fiehn O., Linke T., Willmitzer L. & Fernie A.R.
623 (2001) Metabolic profiling allows comprehensive phenotyping of genetically or
624 environmentally modified plant systems. *The Plant Cell* **13**, 11–29.
- 625 Ross- Davis A.L., Stewart J.E., Hanna J.W., Kim M.-S., Knaus B.J., Cronn R., ...
626 Klopfenstein N.B. (2013) Transcriptome of an *Armillaria* root disease pathogen
627 reveals candidate genes involved in host substrate utilization at the host–pathogen
628 interface. *Forest Pathology* **43**, 468–477.
- 629 Sade D., Shriki O., Cuadros-Inostroza A., Tohge T., Semel Y., Haviv Y., ... Brotman Y.
630 (2014) Comparative metabolomics and transcriptomics of plant response to Tomato
631 yellow leaf curl virus. *Metabolomics* **11**, 81–97.
- 632 Sankaran S., Mishra A., Ehsani R. & Davis C. (2010) A review of advanced techniques for
633 detecting plant diseases. *Computers and Electronics in Agriculture* **72**, 1–13.
- 634 Sarnowska E., Gratkowska D.M., Sacharowski S.P., Cwiek P., Tohge T., Fernie A.R., ...
635 Sarnowski T.J. (2016) The role of SWI/SNF chromatin remodeling complexes in
636 hormone crosstalk. *Trends in Plant Science* **21**, 594–608.
- 637 Scalbert A., Brennan L., Fiehn O., Hankemeier T., Kristal B.S., van Ommen B., ... Wopereis
638 S. (2009) Mass-spectrometry-based metabolomics: limitations and recommendations

639 for future progress with particular focus on nutrition research. *Metabolomics* **5**, 435–
640 458.

641 Sherif M., Becker E.-M., Herrfurth C., Feussner I., Karlovsky P. & Splivallo R. (2016)
642 Volatiles emitted from maize ears simultaneously infected with two *Fusarium*
643 species, mirror the most competitive fungal pathogen. *Frontiers in Plant Science* **7**.

644 Shiokawa Y., Date Y. & Kikuchi J. (2018) Application of kernel principal component
645 analysis and computational machine learning to exploration of metabolites strongly
646 associated with diet. *Scientific Reports* **8**, 3426.

647 Sturrock R.N., Frankel S.J., Brown A.V., Hennon P.E., Kliejunas J.T., Lewis K.J., ... Woods
648 A.J. (2011) Climate change and forest diseases. *Plant Pathology* **60**, 133–149.

649 Stuttmann J., Hubberten H.-M., Rietz S., Kaur J., Muskett P., Guerois R., ... Parker J.E.
650 (2011) Perturbation of arabidopsis amino acid metabolism causes incompatibility with
651 the adapted biotrophic pathogen *Hyaloperonospora arabidopsidis*. *The Plant Cell* **23**,
652 2788–2803.

653 Tschaplinski T.J., Plett J.M., Engle N.L., Deveau A., Cushman K.C., Martin M.Z., ... Martin
654 F. (2014) *Populus trichocarpa* and *Populus deltoides* exhibit different metabolomic
655 responses to colonization by the symbiotic fungus *Laccaria bicolor*. *Molecular plant-
656 microbe interactions* **27**, 546–56.

657 Vinaixa M., Schymanski E.L., Neumann S., Navarro M., Salek R.M. & Yanes O. (2016)
658 Mass spectral databases for LC/MS- and GC/MS-based metabolomics: State of the
659 field and future prospects. *TrAC Trends in Analytical Chemistry* **78**, 23–35.

660 Wong J.W.-H., Lutz A., Natera S., Wang M., Ng V., Grigoriev I.V., ... Plett J.M. (2019) The
661 influence of contrasting microbial lifestyles on the pre-symbiotic metabolite responses
662 of *Eucalyptus grandis* roots. *Frontiers in Ecology and Evolution* **7**, 10.

663 Xu X.-H., Wang C., Li S.-X., Su Z.-Z., Zhou H.-N., Mao L.-J., ... Lin F.-C. (2015) Friend or
664 foe: differential responses of rice to invasion by mutualistic or pathogenic fungi
665 revealed by RNAseq and metabolite profiling. *Scientific Reports* **5**.

666

667 **Tables:**

668 Table 1- The highly-regulated metabolite responses in *E. grandis* root tips after 24 h pre-
669 symbiotic interaction with *A. luteobubalina*

Metabolite	Metabolite class	Mean fold change [†]	p-value
Induced by <i>A. luteobubalina</i>			
Threitol	sugars and sugar alcohols	18.80	0.01*
Tartaric acid	organic acids	13.29	0.09
Trehalose	sugars and sugar alcohols	11.29	0.02*
Mannitol	sugars and sugar alcohols	8.26	0.02*
Unknown_37 (mz = 231, rt = 20.0801)	unclassified	5.55	0.01*
Unknown_50 (mz = 357, rt = 25.0806)	unclassified	2.96	0.12
Unknown_34 (mz = 246, rt = 19.6291)	unclassified	2.29	0.30
Ethanolamine	amino acids and amines	2.27	0.09
Proline	amino acids and amines	2.22	0.16
Unknown_28 (mz = 129, rt = 18.3399)	unclassified	2.22	0.08
Phosphoric acid	other	2.13	0.37
Unknown_52 (mz = 333, rt = 25.2714)	unclassified	2.11	0.05
Unknown_48 (mz = 333, rt = 24.8404)	unclassified	2.08	0.04*
Repressed by <i>A. luteobubalina</i>			
Glyceric acid	organic acids	0.41	0.00*
Unknown_49 (mz = 366, rt = 24.9799)	unclassified	0.41	0.12
Gulonic acid	organic acids	0.41	0.03*
Malic acid	organic acids	0.41	0.04*
Unknown_65 (mz = 446, rt = 28.4172)	unclassified	0.37	0.02*
Unknown_13 (mz = 173, rt = 12.4636)	unclassified	0.37	0.01*
Unknown_35 (mz = 333, rt = 19.7161)	unclassified	0.35	0.01*
Oxalic acid	organic acids	0.32	0.00*
Unknown_26 (mz = 275, rt = 18.1341)	unclassified	0.29	0.08
Shikimic acid	organic acids	0.28	0.00*
Unknown_20 (mz = 159, rt = 16.6234)	unclassified	0.26	0.05*
Pyroglutamic acid	amino acids and amines	0.20	0.00*
Lactic acid	organic acids	0.14	0.08
Threonic acid	organic acids	0.12	0.00*

670 [†] Fold change is calculated in relation to un-inoculated control *E. grandis* root tips.

671 * *p*-value < 0.05

672

673 Table 2- Performance index of the machine learning models used to select potential
674 biomarkers for *Armillaria* infection in *E. grandis*

Machine learning model	Optimized parameters	Performance index			Prediction performance index
		RMSE [†]	R ²	Q ²	AUROC [‡]
RF	mtry = 44	0.1965	0.9605	n.a.	1
rpart	cp = 0.1974	0.1373	0.9445	n.a.	0.9815
sPLSDA	keepX = 4, 4, 5; ncomp = 3	n.a.	0.9064	0.5493	0.8333

675

676 [†]RMSE = Root Mean Square Error

677 [‡]AUROC = Area Under ROC (Receiver operating characteristic)

678 n.a. = not applicable

Author Manuscript

Sample	Unlabelled D-threitol measured quantity (pmole/mg; mean \pm SD)
Root tips after 24 h pre-contact with <i>A. luteobubalina</i> growing in $^{12}\text{C}_6$ -glucose media	126.3 \pm 14.9
Root tips after 24 h pre-contact with <i>A. luteobubalina</i> growing in $^{13}\text{C}_6$ -glucose media	43.4 \pm 12.6
Root tips after 24 h pre-contact with <i>Pisolithus microcarpus</i> growing in $^{13}\text{C}_6$ -glucose media	2.4 \pm 2.8 [†]

[†] D-threitol was measured to be below range for quantitation but within detection limit

681 **Figure legends:**

682 **Figure 1:** Volcano plot shows differential metabolite responses of *E. grandis* root tips
683 towards *A. luteobubalina* pre-symbiotic interaction (n = 8) in comparison to untreated control
684 root tips (n = 4). The x-axis and y-axis explain the log₂-transformed fold change and the
685 significance of the fold change in form of -log₁₀ p-value, respectively. Each point represents a
686 type of metabolite detected by GC-MS untargeted metabolite profiling, with the colour of the
687 points represent the classification of the metabolites. Significantly differential metabolite
688 responses ($|\log_2\text{fold change}| > 2$ and p-value < 0.05) are labelled in the plot.

689

690 **Figure 2:** Scatter plot matrix demonstrates the dispersion of overall metabolite profiles for *E.*
691 *grandis* root tips under pre-symbiotic interaction with five distinct microbial species. The plot
692 describes the correlation of the first four principle components (PCs) of the PCA. Each point
693 represents the metabolite profile of a *E. grandis* root tips sample, with the color representing
694 a different microbial treatment.

695

696 **Figure 3:** (a) The variable importance of the top-ten metabolite responses selected by three
697 MS models. The variable importance is an indicator of the predictive power of the metabolite
698 responses in discriminating between the three classifiers: *A. luteobubalina*-treated roots
699 (Armi), untreated control roots (Ctrl) and roots treated with other microbial species (Other).
700 (b-c) The boxplot and scatter matrix plot showing the normalized metabolite responses of
701 threonic acid, lactic acid, threitol, shikimic acid and inositol across three classification groups.
702 These five metabolite responses were commonly selected by all three MS models with the
703 best predictive powers.

704

705 **Figure 4:** The threitol response of root tips towards *Armillaria* in pot soil-based sample in
706 comparison to mock-inoculated control condition. The threitol response is normalized by
707 dividing the detected peak corresponding to threitol by the weight of root tip samples,
708 followed by log-transformation and auto-scaling. The difference in threitol response is
709 significant with p-value = 0.031.

710

711 **Figure 5:** Distribution of different isotopomers of threitol detected across a set of *A.*
712 *luteobubalina* fungal mycelium samples (FM) and the interacting root tip samples (RT) in
713 labelled and unlabeled control condition. The proportion of each isotopomer of threitol is
714 calculated by dividing the detected intensity with the combined intensities of all detectable
715 isotopomers. The shade of grey represent different isotopomers of derivatized threitol with
716 distinct m/z values : unlabeled threitol (m/z = 217), ¹³C₁-threitol (m/z = 218), ¹³C₂-threitol
717 (m/z = 219), ¹³C₃-threitol (m/z = 220) and ¹³C₄-threitol (m/z = 221).

718

719 **Figure 6:** Quantification of threitol level (a) and cell damages as represented in form of
720 electrolytes leakage (b) in *E. grandis* root tissues (black line) and in *A. luteobubalina* fungal
721 mycelia tissues (grey line) over the timecourse of interaction. Threitol levels (ppm) are
722 expressed as means ± standard error (SE). Different letters indicate significant differences (p-
723 value < 0.05) among different time points. (c) Quantification of threitol level in *A.*
724 *luteobubalina* fungal mycelia grown in PDA media of different strength. Asterisks indicate
725 statistically significant differences (p-value < 0.001, one-way ANOVA).

726

727 **Figure 7:** Effect of threitol enrichment at 0.3ppm and 12ppm levels on the interaction of *E.*
728 *grandis* with different microbes. The bar-graphs depicts the percentage of root lesion caused
729 by *A. luteobubalina* (a) and *Ph. cinnamomi* (b), as well as the percentage of root colonization
730 by *P. microcarpus* (c). Data points are means ± SE. Different letters indicate significant
731 differences (p-value < 0.05) among different threitol levels.

732

733 **Figure 8:** Fold change corresponding to the expression of nine marker genes responsive
734 towards different hormones (shown in bracket) in *E. grandis* roots after 1 d exposure to
735 threitol (a) and to inositol (b). Fold changes of these genes are log₂-transformed and shown in
736 comparison to 0ppm control condition. Data points are means ± SE. Asterisk (*) above the
737 bars indicate the significance of the gene expression changes in relation to the 0 ppm control
738 condition (*p-value < 0.05, **p-value < 0.01, ***p-value < 0.001).

739

740 **Additional Files:**

741 **Supplementary Materials and Methods:** This document details the analytical procedures
742 for Untargeted metabolite profiling, ¹³C enrichment analysis as well as targeted quantitation
743 of threitol in samples used in this study.

744

745 **Figure S1:** Schematic diagram of the workflow for the machine learning models used in this
746 study for selecting the important and specific metabolite responses for *A. luteobubalina* in *E.*
747 *grandis* roots during pre-symbiotic interaction. parRF = parallel random forest; rpart =
748 recursive partitioning; sPLSDA = sparse partial least square discriminative analysis.

749

750 **Table S1:** Isolates of fungi and oomycete, and their respective growth medium used in this
751 study.

752

753 **Table S2:** Primer sequences used in the RT-qPCR assay.

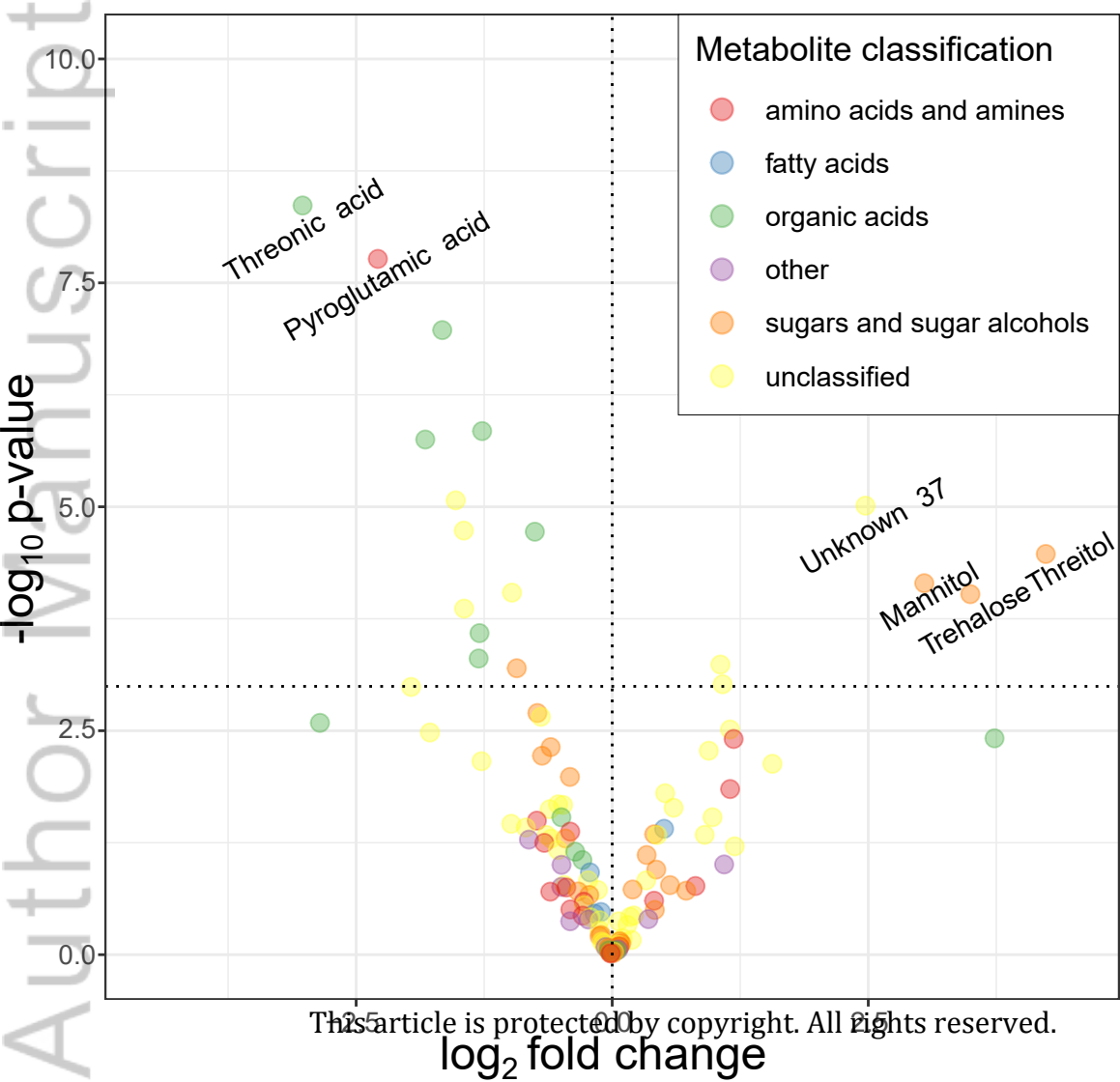
754

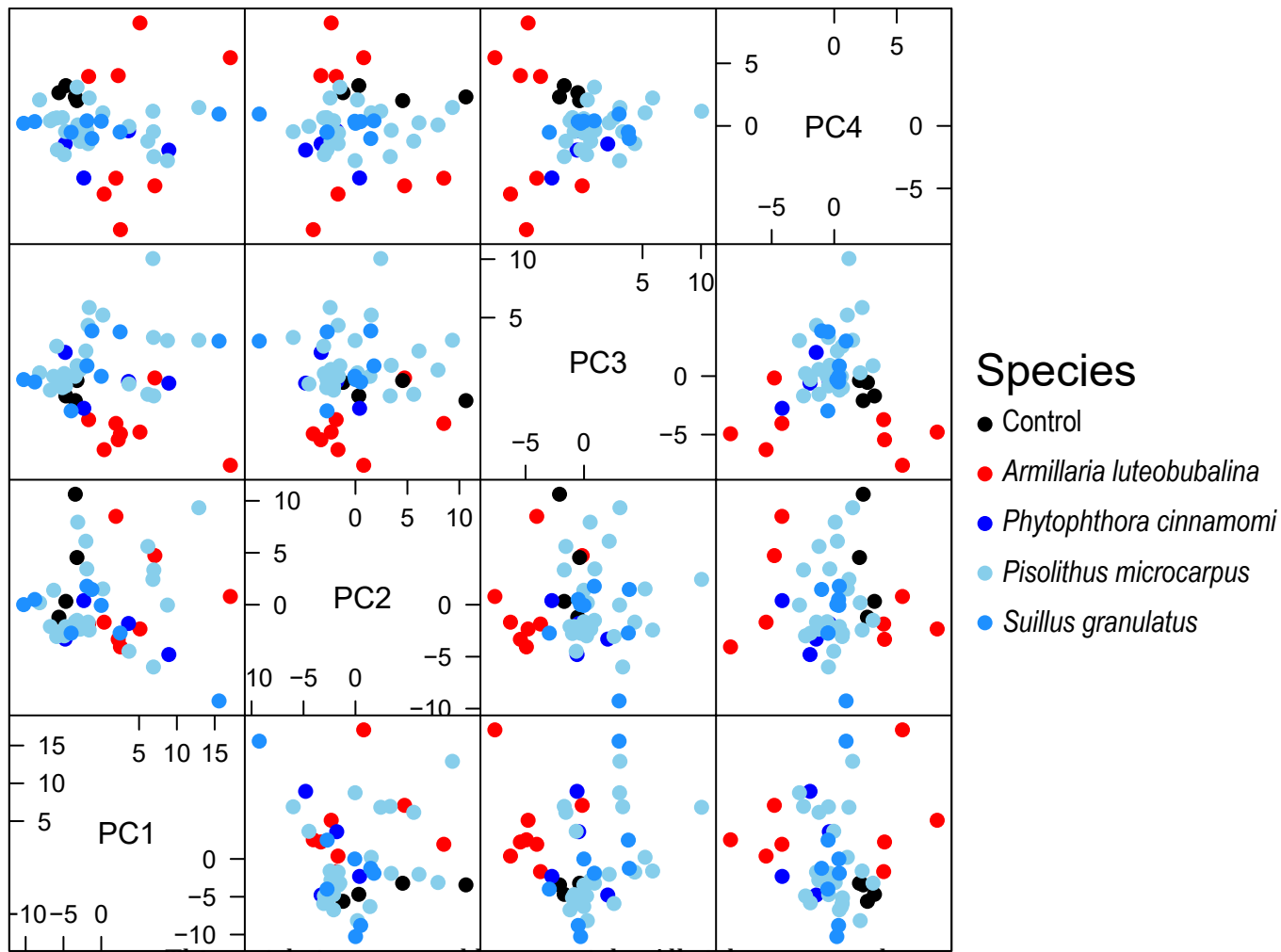
755 **Table S3:** Metabolite profiling data matrix containing the relative metabolite responses of *E.*
756 *grandis* roots after pre-symbiotic interaction with different species of microbes.

757

758 **Table S4:** Root metabolite responses after 24 h pre-symbiotic interaction with *A.*
759 *luteobubalina*. The fold-change and the *p*-value of each metabolite response, as well as their
760 metabolite classes are provided in the table.

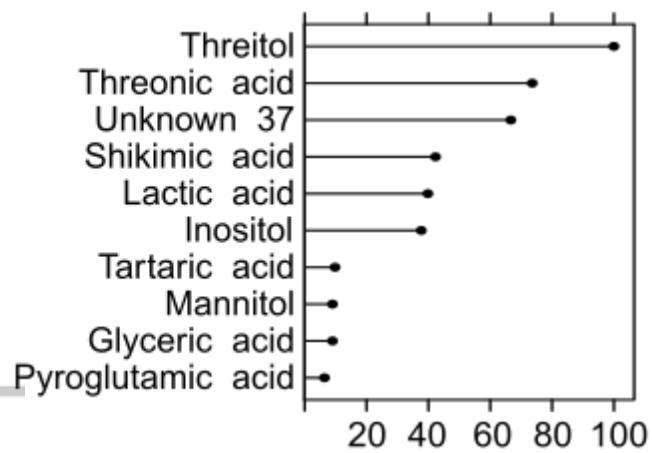
761



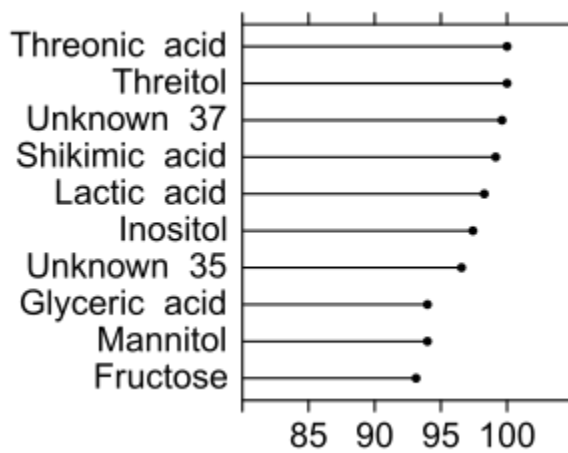


(a)

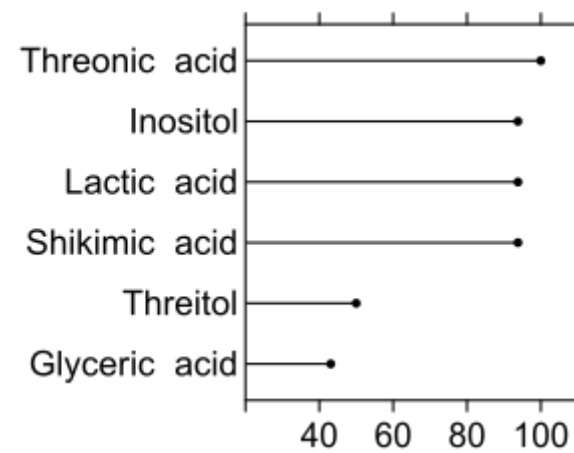
parRF



sPLSDA

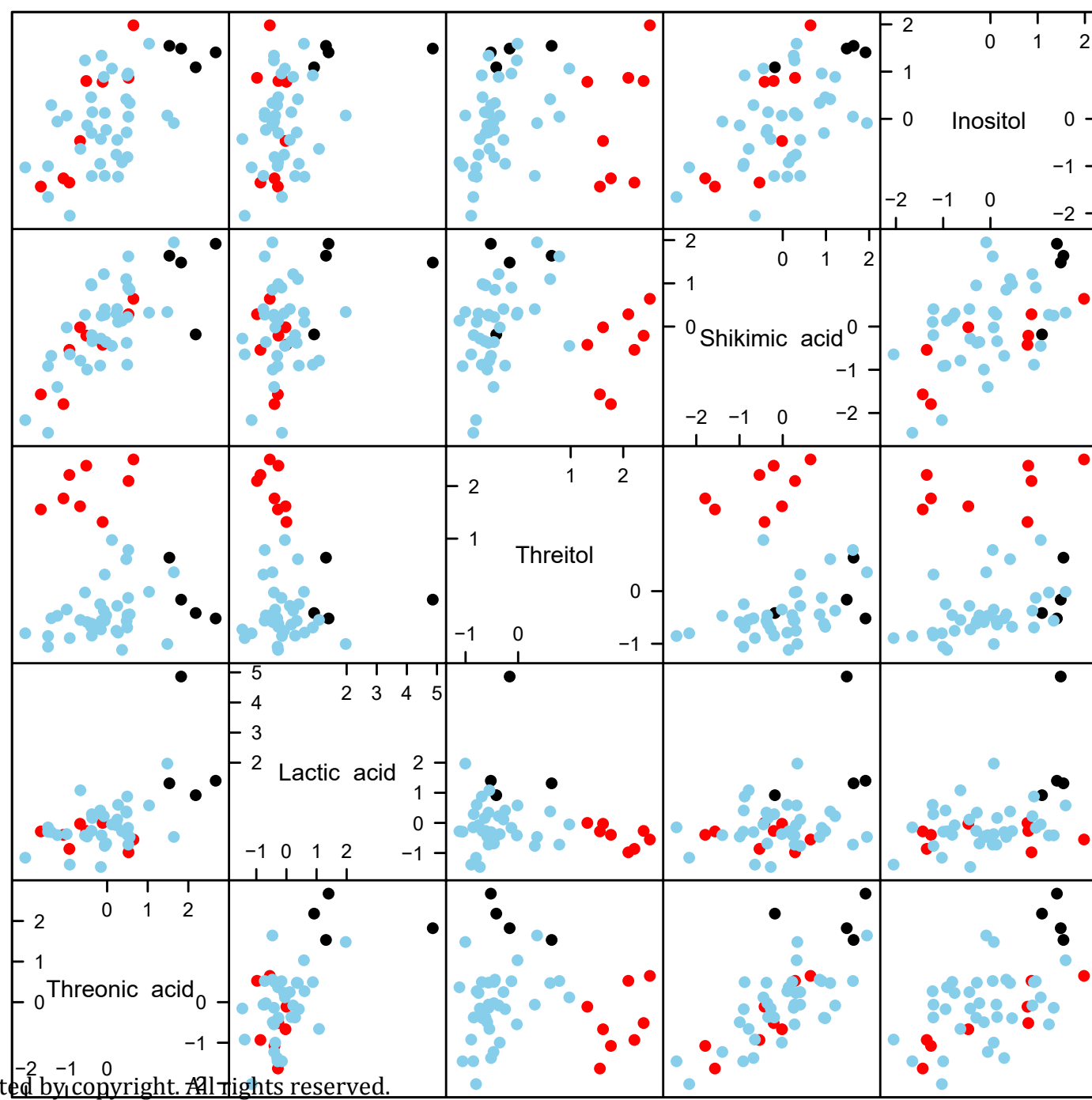
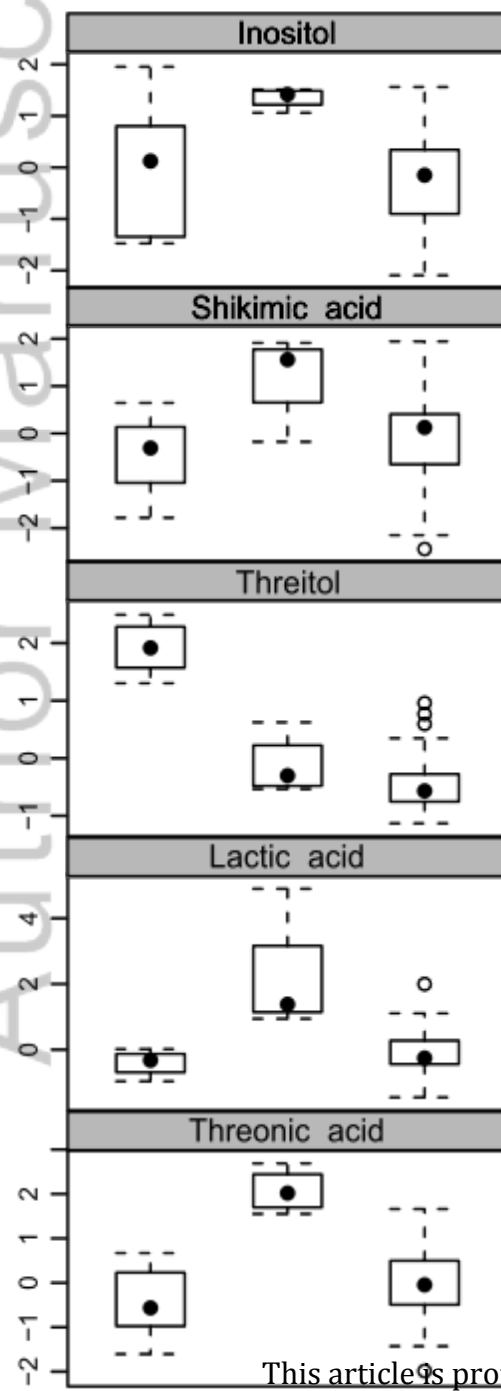


rpart



(b)

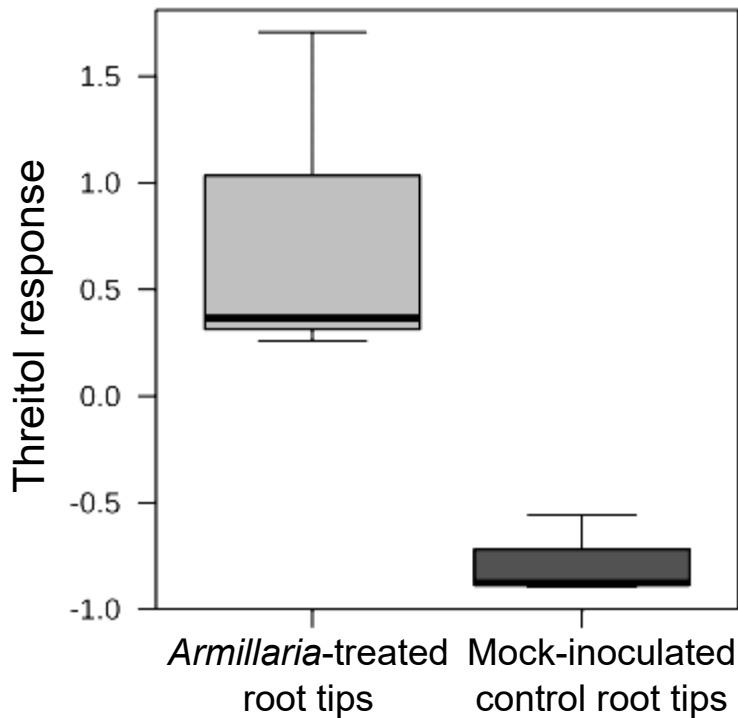
(c)

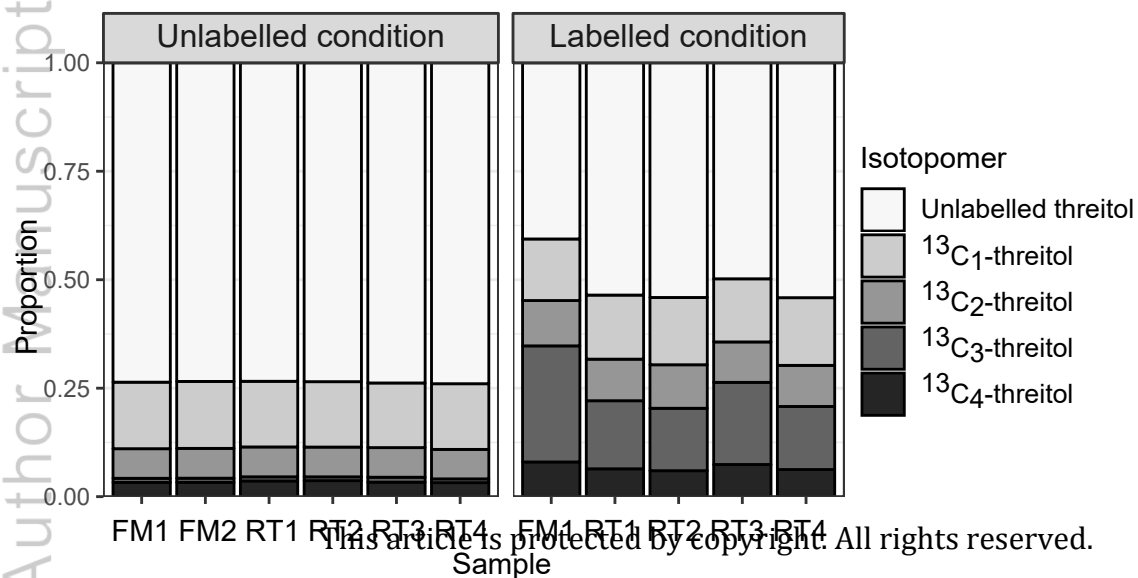


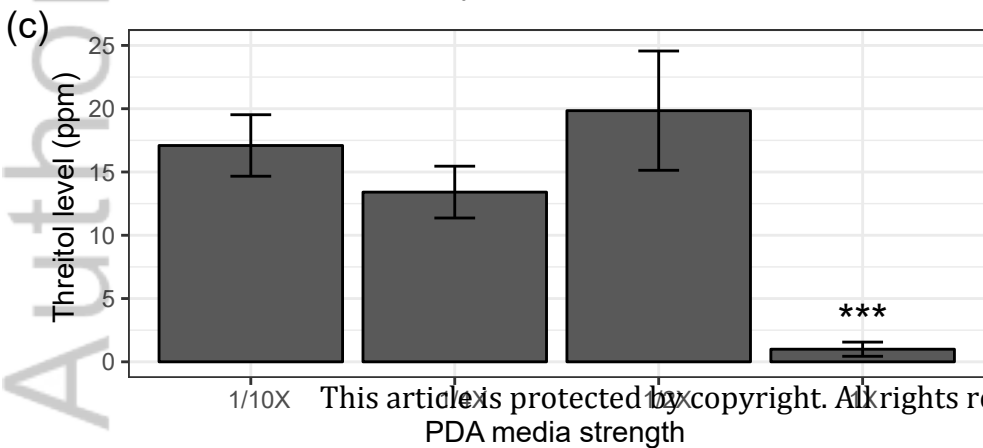
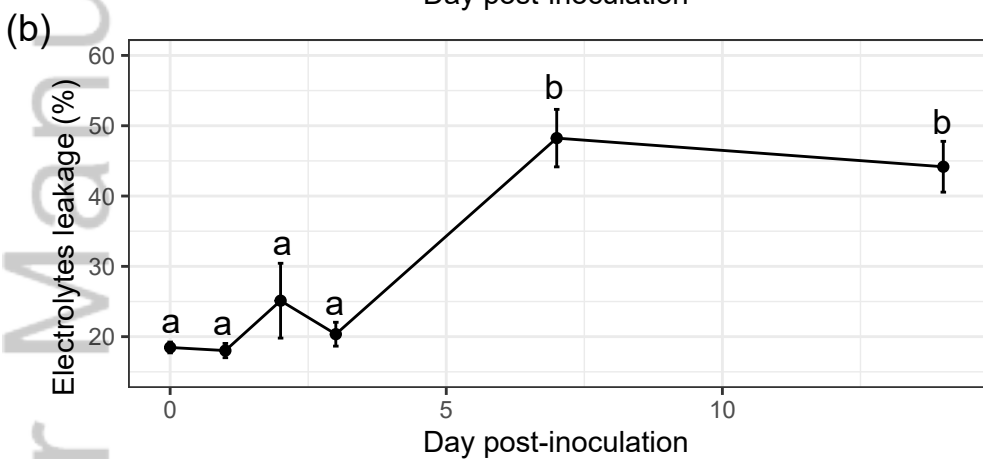
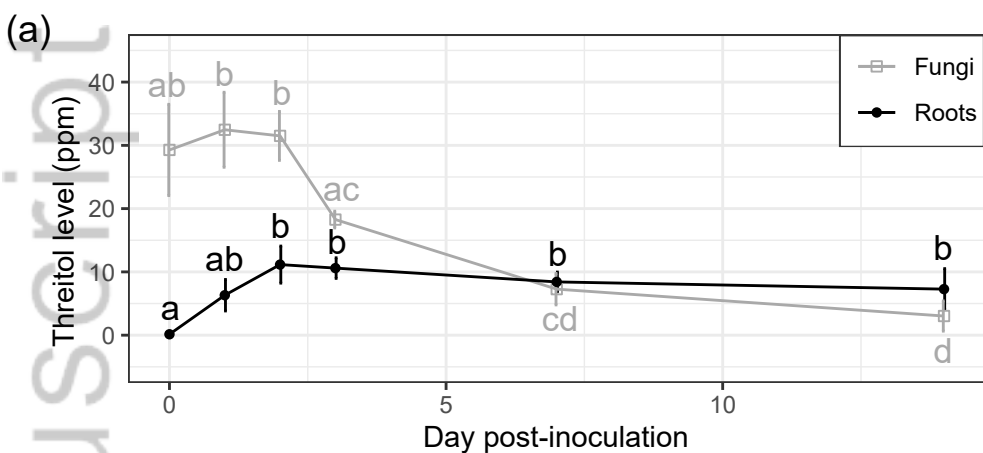
This article is protected by copyright. All rights reserved.

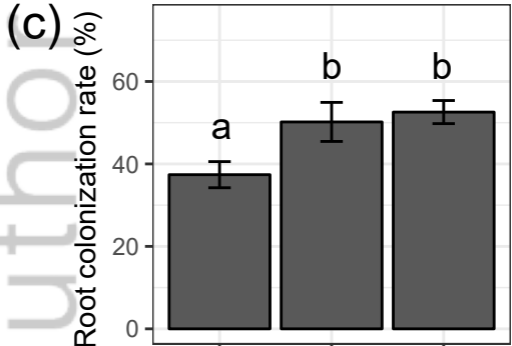
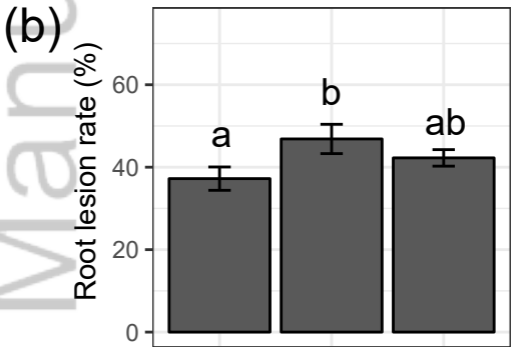
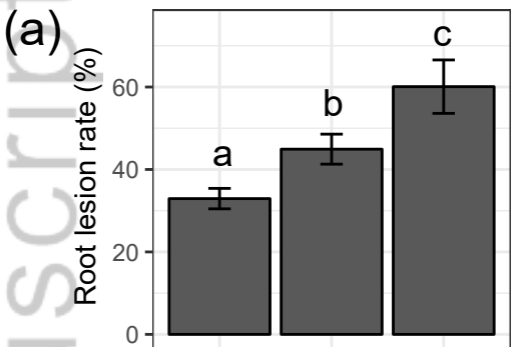
Armillaria Control Other

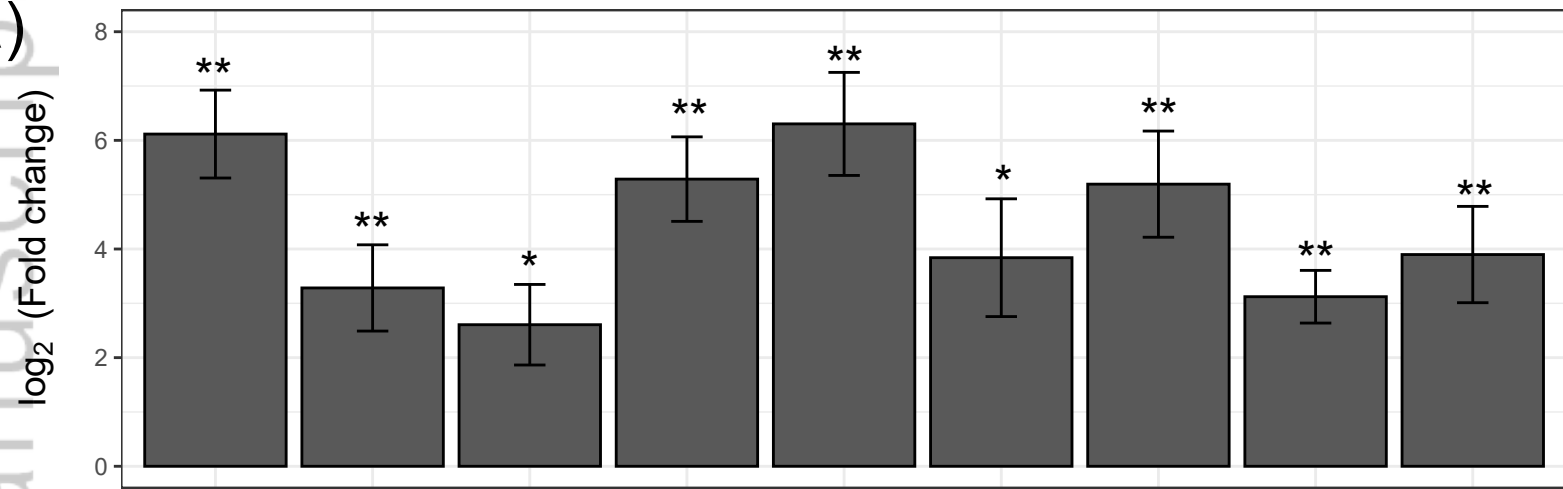
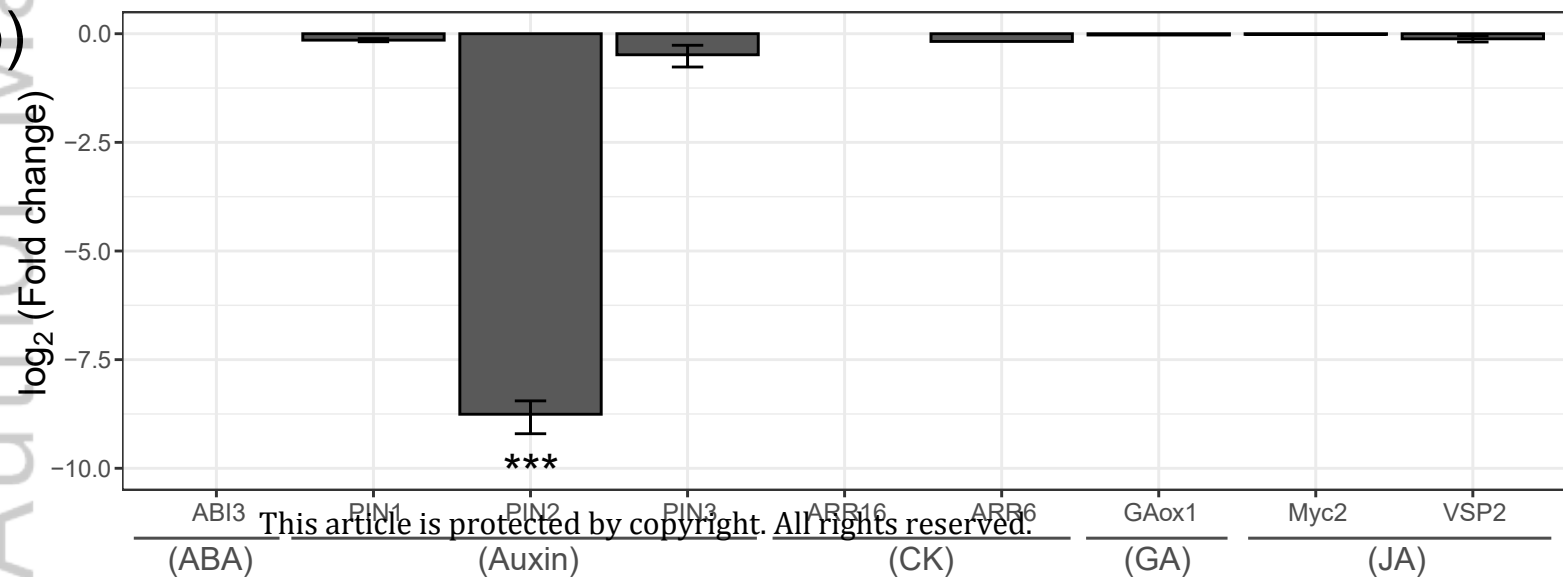
● Armillaria ● Control ● Other









(a)**(b)**

This article is protected by copyright. All rights reserved.

(ABA)

(Auxin)

(CK)

(GA)

(JA)